Carbohydrate Polymers 115 (2015) 478–484

Contents lists available at ScienceDirect

Carbohydrate Polymers

journal homepage: www.elsevier.com/locate/carbpol

Comparison between the interactions of the cationic surfactant DODAB with xanthan and galactomannan

Gabriel A.T. Kaminski[a,b], Maria Rita Sierakowski[a], Roberto Pontarolo[b], Rilton Alves de Freitas[a,*]

[a] BioPol Laboratory, Chemistry Department, Federal University of Paraná, R. Coronel F. H. dos Santos 210, 81531-980 Curitiba, Paraná, Brazil
[b] CEB, Pharmacy Department, Federal University of Paraná, Av. Prof. Lothário Meissner 3400, 80210-170 Curitiba, Paraná, Brazil

ARTICLE INFO

Article history:
Received 14 April 2014
Received in revised form 25 August 2014
Accepted 27 August 2014
Available online 18 September 2014

Keywords:
DODAB
Xanthan
Galactomannan
Cationic surfactant
Natural polymer
Interaction

ABSTRACT

The interactions of the cationic surfactant DODAB with anionic xanthan (XAN) and nonionic galactomannan (GMC) polysaccharides in solution were investigated using tensiometry, differential scanning microcalorimetry (μ-DSC), zeta potential and dynamic light scattering (DLS) techniques and by the calculated thermodynamic parameters of ΔG^0_{ves}, ΔG^0_{ads}, Γ_{max} and a_{min}. The surfactant formed large unilamellar vesicles (LUV) that aggregated with both the polymers in solution. Increasing DODAB concentrations resulted in greater and greater DODAB–XAN aggregates, high turbidity and even precipitation, while DODAB–GMC aggregates remained equal sized, clear solution and no precipitation observed. Further addition of DODAB to XAN solution was able to resuspend the precipitates. The interactions with both polysaccharides resulted in a more spontaneous adsorption of the DODAB–polymer aggregates at the air/solution interface with lower surfactant population.

1. Introduction

The interactions between ionic surfactants and natural polymers have been studied and have shown promise for applications such as designing functional nano-objects. These nanofabrication techniques have potential for use in drug delivery, functionalization, sensors, membranes and biomedicine. In aqueous solution, polymers and surfactants show synergistic behavior, with substantially reduced surface tensions compared with the surface tension of pure surfactant (Jiang, Wang, Yang, & Lin, 2013).

Surfactant–polymer interactions minimize the total amount of surfactant necessary for many industrial applications; thus, they can be used to reduce process costs as well as environmental impact. However, there have been few investigations on the interactions of cationic surfactants with polymers (Dal-Bó, Laus, Felippe, Zanette, & Minatti, 2011). The role of cationic surfactants as drug carriers has increased in many pharmaceutical applications, such as the development of gene therapies, and its interactions with natural polymers might be a promising tool for delivery systems.

Dioctadecyldimethylammonium bromide (DODAB) is a cationic surfactant with a quaternary ammonium salt as its polar head group and two 18-carbon saturated chains. The gel to liquid–crystalline phase transition, also known as melting temperature (T_m), is 45 °C. Vesicles are not spontaneously formed below this temperature because the surfactant is poorly soluble. However, once the vesicles are formed, above T_m, they remain stable even at temperatures as low as 5 °C for months (Feitosa, Jansson, & Lindman, 2006; Wu, Yu, & Ji, 2011).

In this manuscript we evaluate the interactions between DODAB and the natural polymers, which have a synergistic interaction between themselves, xanthan (XAN) and galactomannan (GMC). XAN is an anionic biopolymer produced by *Xanthomonas campestris* that is composed of a (1→4)-β-D-glucan cellulose backbone substituted with an acid trisaccharide in the side chain (Jansson, Kennark, & Lindberg, 1975). GMC is a neutral water soluble biopolymer from *Ceratonia siliqua* seeds that is composed of a (1→4)-β-*D*-mannan backbone with (1→6)-α-D-galactose substitutions (Dea & Morrison, 1975).

Surfactants form aggregates upon binding to polymers at the critical aggregation concentration (CAC), which is lower than the critical vesicle concentration (CVC) of the surfactant alone. Above the CAC, the formation of pure surfactant vesicles occurs; the concentration at which this happens is known as the second critical concentration and is a higher concentration than the CVC in a solution of pure surfactant (Chakraborty, Chakraborty, & Ghosh, 2006).

With charged polymers, aggregates are formed and sustained by electrostatic interactions between the polar head groups of the polymer and the surfactants and are reinforced by the hydrophobic

* Corresponding author. Tel.: +55 41 3361 3260; fax: +55 4133613186.
E-mail addresses: rilton@quimica.ufpr.br, rilton@pq.cnpq.br (R.A.d. Freitas).

http://dx.doi.org/10.1016/j.carbpol.2014.08.111
0144-8617/

interactions between the alkyl chains of the bound surfactant molecules. Surfactants aggregate on neutral polymers because of the hydrophobic interactions between the apolar tails of the surfactant and the polymer backbone (Bain et al., 2010).

The interactions between cationic dimethyldioctadecylammonium bromide (DODAB) with anionic XAN and neutral GMC were investigated using tensiometry, differential scanning microcalorimetry (μ-DSC), zeta potential and dynamic light scattering (DLS) techniques and by the calculation of thermodynamic parameters.

2. Materials and methods

2.1. Polymer purification and characterization

Xanthan gum (Sigma-Aldrich, Switzerland) was purified by dialysis through a cellulose membrane with 12 kDa pores (Sigma-Aldrich, Switzerland). The sample was lyophilized (Thermo-Fisher Scientific, USA) after purification with 0.1 mol L^{-1} acetic acid for 3 days to ensure that all the molecules would be in a molecular conformation, followed by purification with ultrapure water with a conductivity of <2 μS cm^{-1} (Millipore MilliQ-System, USA) for 2 days to remove the acetic acid.

Locust bean galactomannan gum from *C. siliqua* seeds (Sigma-Aldrich, Switzerland) was purified by heating–solubilization in ultrapure water and centrifugation at 10,000 g for 20 min at 40 °C in a 4K15C centrifuge (Sigma, Germany). Ethyl alcohol (99%) was added to the supernatant to achieve a 70% alcohol concentration, and then, this suspension was centrifuged at 10,000 g for 20 min at 5 °C to separate the purified GMC. The polymer was washed with 99% ethyl alcohol and then centrifuged as described above and dried at 40 °C under vacuum.

The polymers, at a concentration of 0.5 mg mL^{-1}, were characterized by steric exclusion chromatography (SEC) with 0.1 mol L^{-1} $NaNO_3$ and 200 ppm sodium azide as the mobile phase at 0.4 mL min^{-1}. The system was composed of a UV/Vis detector, a refractometer, a light scattering detector at 7° and 90° and a differential viscometer detector (Viscotek, USA) with a OHpak SB-806M HQ (Shodex, USA) column at 40 °C.

The zeta potential was determined for 0.5 mg mL^{-1} polymer solution in ultrapure water, with or without DODAB, by the electrophoretic mobility, measured on a Zetasizer Nano-ZS (Malvern, USA) in disposable cuvettes at 25 °C with 120 s of stabilization.

2.2. Surfactant and polymer interactions

2.2.1. Sample preparation

In order to ensure that the surfactant chains were melted and, therefore, DODAB molecules were soluble in all analyses so that the interactions measured were between free surfactant molecules with polymers and not surfactant vesicles, all samples were prepared as follows. DODAB (Sigma-Aldrich, Switzerland) purity > 98%, was added to ultrapure water and kept in a sealed tube at 80 °C for 24 h and this mixture was vortexed several times. Only after this procedure further dilution in ultrapure water or polymer solution took place.

2.2.2. Tensiometry

The surface tension was determined by the pendant drop method in a OCA15+ (DataPhysics, Germany) device, which calculates the interfacial tension in real time with the Laplace–Young equation using the SCA20 software. DODAB was weighed and added to ultrapure water for a final concentration of 10,000 μmol L^{-1} and followed sample preparation as described above. Drops were formed with a volume of 0.1 μL less than the volume necessary to trickle and analyzed by tracking mode for 700 s.

The diffusion time for DODAB was determined by the Einstein–Smoluchowski equation, and the tridimensional migration time to the interface for all surfactant molecules was calculated to be approximately 670 s. The tensiometric results shown are the median values registered at the plateau between 600 and 700 s in each experiment.

2.2.3. Zeta potential

The samples prepared for tensiometry were analyzed with an electrophoretic mobility zeta potential analysis on a Zetasizer Nano-ZS (Malvern, USA) using disposable cuvettes at 25 °C.

2.2.4. Dynamic light scattering (DLS)

The samples prepared for tensiometry were analyzed with dynamic light scattering with angle detection at 173° in a Zetasizer Nano-ZS (Malvern, USA) using disposable cuvettes at 25 °C.

2.2.5. Differential scanning calorimetry (μ-DSC)

Experiments were performed in a Micro DSC III (Setaram, France) microcalorimeter under a nitrogen atmosphere with 10 bar continuous flow using 1 cm^3 vessels with a heating and cooling rate of 0.2 °C min^{-1}. The data were collected with the Setsoft 2000 software. DODAB, at a final concentration of 5 mmol L^{-1}, was added to a 0.5 mg mL^{-1} solution of XAN in ultrapure water, as described previously.

2.2.6. Thermodynamic parameters of vesicle formation and adsorption

The standard free energy of vesicle formation (ΔG^0_{ves}) in J mol^{-1} was calculated using Eq. (1) (Berg, 2010),

$$\Delta G^0_{ves} = (1+\beta)RT\ln\frac{[n\,\text{mols DODAB}]}{[n\,\text{mols solvent} + n\,\text{mols DODAB}]} \quad (1)$$

where β is the apparent degree of counterion binding to the vesicle/solution interface and is calculated with 1–α, where α is the apparent degree of counterion dissociation from the vesicle/solution interface. The degree of ionization of DODAB was determined to be 0.4 by conductivity titration (data not shown).

The maximum surface excess at the air/solution interface (Γ_{max}) in mol m^{-2} was calculated by applying the Gibbs adsorption isotherm (Berg, 2010),

$$\Gamma_{max} = \frac{-1}{2.303RT}\left(\frac{\partial\gamma}{\partial\log c}\right)_T \quad (2)$$

The minimum area occupied by a surfactant molecule at the air/solution interface (a_{min}) in nm^2 was estimated using Eq. (3) (Berg, 2010),

$$a_{min} = \frac{10^{18}}{N_A\Gamma_{max}} \quad (3)$$

where N_A is Avogadro's number.

The standard free energy of adsorption (ΔG^0_{ads}) in J mol^{-1} at the air/solution interface was evaluated using the Eq. (4) (Rosen & Aronson, 1981),

$$\Delta G^0_{ads} = \Delta G^0_{ves} - 0.6023\pi_{cvc}a_{min} \quad (4)$$

where π_{cvc} in J m^{-2} is the surface pressure at the CVC and was calculated using the difference between the surface tension of water or polymer solution and the surface tension of the surfactant solution at the CVC in water or the polymer solution.

Table 1
Physicochemical characteristics of the polymers and the surfactant: molar mass (M_w), radius of gyration (R_g) and zeta potential (ζ-potential).

Molecule	M_w (g mol^{-1})	R_g (nm)	ζ-potential (mV)
XAN	1.03×10^6[a]	69[a]	−54.1 (±7.7)[c]
GMC	0.26×10^6[a]	52[a]	−5.4 (±6.2)[c]
DODAB	630[b]	–	+66.5 (±9.4)[c]

[a] Determined by GPC using 0.1 mol L^{-1} $NaNO_3$ and 200 ppm sodium azide as the mobile phase at 0.4 mL min^{-1} at 40 °C through a Shodex OHpakSB-806 HQ column.
[b] According to the manufacturer.
[c] Determined by electrophoretic mobility in ultrapure water at 25 °C.

3. Results

3.1. Characterization of the polymers

The purified polymers exhibited an unimodal distribution as measured by GPC (data not shown). The physicochemical characteristics of GMC, XAN and DODAB are presented in Table 1.

3.2. Tensiometry

Fig. 1a shows the tensiometry results for DODAB in ultrapure water and in solutions of XAN and GMC at 0.5 mg mL^{-1}. High interfacial tension plateaus are observed at more dilute surfactant concentrations, whereas lower plateaus are observed at higher concentrations. The precipitation region that is indicated applies only to DODAB in XAN solution; precipitation is not observed in ultrapure water or GMC solution. The bars denote the standard deviation of triplicates.

3.3. Zeta potential

Fig. 1b shows the zeta potential analysis for DODAB in ultrapure water and in solutions of GMC and XAN at 0.5 mg mL^{-1}. An increase in the zeta potential is observed with higher surfactant concentration in all the mixtures, as expected. The bars denote the standard deviation of triplicates.

3.4. Dynamic light scattering (DLS)

Fig. 1c shows the diameter of the DODAB aggregates in ultrapure water and in solutions of GMC and XAN at 0.5 mg mL^{-1}. Nanoparticle formations are observed in all of the mixtures (Supplementary files 1 and 2). The bars denote the standard deviation of triplicates.

3.5. Thermodynamic parameters of adsorption and vesicle formation

The μ-DSC (Fig. 2) analysis showed that the interaction between DODAB and XAN magnified the enthalpy of the DODAB transition event at the same temperature found by Brito and Marques (2005), from 16 J mol^{-1} to 80 J mol^{-1}, which is a five-fold increase.

The exothermic observed event is related to the surfactant liquid crystalline–gel transition, since Fig. 2 shows the cooling curves. The magnification of the enthalpy in the presence of XAN might be due to better accommodation of the DODAB molecules on the polymer

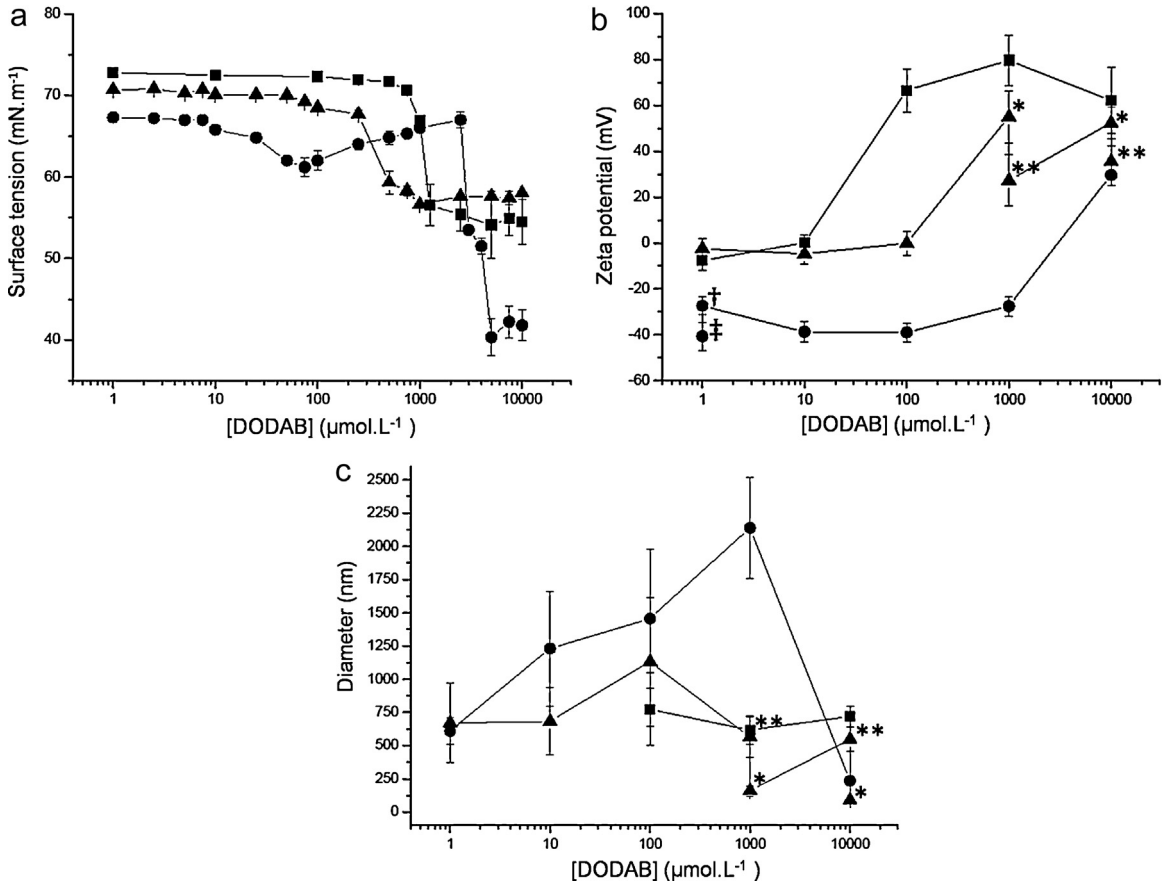

Fig. 1. (a) The tensiometric isotherm, as determined by pendant drop. (b) The zeta potential, as determined by electrophoretic mobility. (c) The hydrodynamic diameter as determined by dynamic light scattering. DODAB in ultrapure water (■) in GMC (▲) at 0.5 mg mL^{-1} and XAN (●) at 0.5 mg mL^{-1}. All experiments were carried out at 25 °C. Bimodal distributions were observed: * Relative to Free DODAB vesicles. ** Relative to DODAB-GMC aggregates. † Relative to DODAB-XAN aggregates. ‡ Relative to free XAN molecules. The bars denote the standard deviation of triplicates.

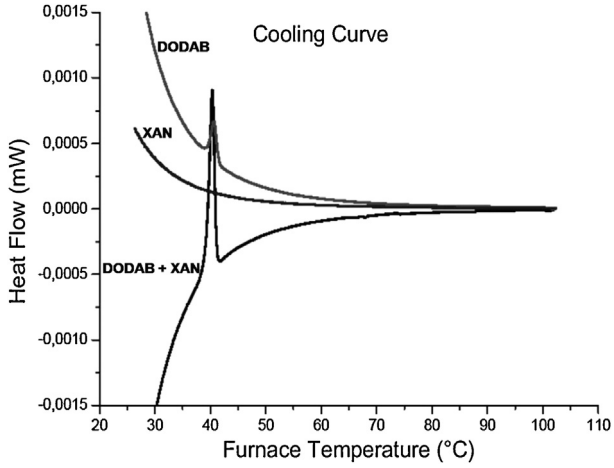

Fig. 2. Differential scanning microcalorimetry analyses showing the systems were composed of LUV. The highest line represents 5 mmol L^{-1} DODAB in ultrapure water; the line in the middle represents XAN solution without DODAB; the lower line represents 5 mmol L^{-1} DODAB in XAN solution at 0.5 mg mL^{-1}. Experiments were performed under a nitrogen atmosphere with 10 bar flow at heating and cooling rate of 0.2 °C min^{-1}.

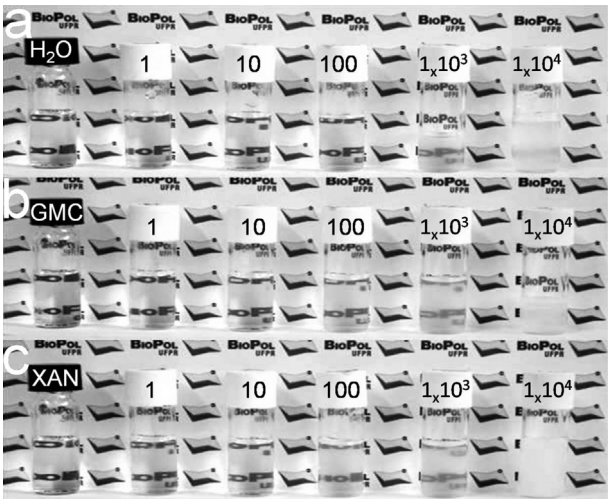

Fig. 3. (a) DODAB in ultrapure water, (b) GMC solution at 0.5 mg mL^{-1} and (c) XAN solution at 0.5 mg mL^{-1}. The black lids indicate the solutions without surfactant. The numbers on the white lids indicate the concentration of DODAB in μmol L^{-1}. In the case of DODAB at 100 and 1000 μmol L^{-1} in XAN solution the flasks contain only the supernatant.

molecules, leading to more stability and overall organization of the system.

All the analyzed systems formed LUV, since there was only one event (data not shown) in the heating curve at ~45 °C, the gel-to-liquid crystalline temperature known as T_m, and one event at the cooling curve at ~40 °C = T'_m, with a $\Delta T_m = 5$ °C thermal hysteresis characteristic to LUV systems (Feitosa, Barreleiro, & Olofsson, 2000). Feitosa, Adati, Hansson, and Malmsten (2012) found that the thermal analysis of DODAB 5 mmol dispersed in water only with magnetic stirring resemble those of DODAB 1 mmol which are composed majorly by LUV.

Other thermodynamic parameters were calculated and are presented in Table 2. They are the standard free energy of vesicle formation (ΔG^0_{ves}), the standard free energy of adsorption (ΔG^0_{ads}), the maximum surface excess at the air/solution interface (Γ_{max}), and the minimum area occupied by a surfactant molecule at the air/solution interface (a_{min}). These parameters provide a better understanding of the cationic surfactant molecules' behavior in the presence and absence of anionic xanthan and nonionic galactomannan polymer molecules, as described in the discussion section.

Fig. 3 shows solutions of DODAB at different concentrations in ultrapure water and in solutions of GMC and XAN. Different degrees of turbidity are observed.

4. Discussion

4.1. Polymer characterization

After purification, XAN had the expected molecular weight (M_w), intrinsic viscosity and radius of gyration (R_g) (Gulrez, Al-Assaf, Fang, Phillips, & Gunning, 2012). The purified GMC had a lower M_w and R_g than those observed by Dakia, Blecker, Robert, Wathelet, and Paquot (2008), as observed in Table 1. After purification, a fraction was obtained from the GMC solution that had a 1:3.5 molar ratio of galactose to substituted mannose, as determined by NMR (data not shown). The small negative charge on the GMC polymer might be caused by attached proteins that remain even after polymer precipitation with ethyl alcohol.

4.2. Evaluation of the DODAB–GMC interaction data

Fig. 1a shows that in solutions of GMC, the interfacial tension starts to decrease at lower concentrations of DODAB relative to the concentrations in ultrapure water. This indicates that DODAB–GMC aggregates have formed and migrated to the air/water interface. These aggregates exhibit surface activity; therefore, fewer surfactant molecules are necessary to reduce the interfacial tension. Although the interfacial tension decreases at lower DODAB concentrations in a solution of GMC, the CVC plateau is reached at a similar DODAB concentration to that in ultrapure water so that it becomes impossible to differentiate between the CAC and the CVC.

The higher surface tension plateau at the CVC for DODAB in a solution of GMC can be attributed to hindrance effects of the aggregates, which have already been described for interactions between cationic surfactants and nonpolar polymers (Manoli & Avranas, 2013; Manousakis & Avranas, 2013). The interaction between DODAB and GMC is sustained mainly by hydrophobic forces. The surfactant tails bind to the polymer backbones; this binding reduces the need for adsorption because the aggregates that are formed have exposed polar ammonium heads and can thus be better stabilized in the bulk.

As the surfactant molecules interact with the GMC, the aggregates increase in zeta potential (Fig. 1b) and diameter (Fig. 1c). Above the CVC there is a bimodal distribution, indicating that the GMC interaction sites are saturated and the surplus of surfactant molecules results in the formation of pure DODAB vesicles. The decrease in the diameter of the DODAB–GMC aggregates at higher DODAB concentrations can be attributed to shrinkage due to the Coulombic repulsion between the vesicles and the aggregates, which is a result of the fact that the whole system is now positively charged.

DODAB interacts with GMC mainly by hydrophobic interactions between the alkyl tails of the DODAB and the polymer backbones. Hence, the surfactants' positively charged ammonium groups face outward, and their Coulombic repulsion inhibits more DODAB molecules from binding to the polymer molecules.

In the tensiometric profile of DODAB in GMC solution (Fig. 1a), the surface tension starts to decrease at approximately 100 μmol L^{-1}, and the interface saturation occurs at approximately 1000 μmol L^{-1}.

Table 2
Thermodynamic parameters calculated showing the DODAB, GMC and XAN interactions.

Themodynamic parameters	DODAB in water	DODAB + GMC	DODAB + XAN	
		Aggregation + Free vesicles	Aggregation	Free vesicles
CVC ($mol\,L^{-1}$)	5.5×10^{-4}	–	–	16.4×10^{-4}
CAC ($mol\,L^{-1}$)[a]	–	8.6×10^{-4}	6.2×10^{-4}	–
ΔG^0_{ves} ($kJ\,mol^{-1}$)	−39.9	−46.4	−39.6	−36.2
ΔG^0_{ads} ($kJ\,mol^{-1}$)	−78.5	−143.5	−478.4	−79.8
Γ_{max} ($mol\,m^{-2}$)	4.7×10^{-6}	1.4×10^{-6}	5.9×10^{-7}	5.9×10^{-6}
a_{min} (nm^2)	3.5	12.0	28.4	2.8

CVC is the critical micelle concentration; CAC is the critical aggregation concentration; and ΔG^0_{ves} and ΔG^0_{ads} are the free energy of vesicle formation and adsorption, respectively. Γ_{max} is the maximum surface excess, and a_{min} is the minimum area occupied by a surfactant molecule, both at the air/solution interface.

4.3. Evaluation of the DODAB–XAN interaction data

As observed in the tensiometric interaction profiles (Fig. 1a), in the XAN solution, the surface tension starts to decrease at lower surfactant concentrations than in the other mixtures. It reaches a plateau between 50 and 100 $\mu mol\,L^{-1}$ of DODAB and then rises again up to 1250 $\mu mol\,L^{-1}$ before abruptly dropping at higher concentrations. It was also observed that precipitation occurred only in the XAN solution between concentrations of 25 and 1250 $\mu mol\,L^{-1}$; the high turbidity of this system in comparison with the other mixtures is shown in Fig. 3.

The reduction in the interfacial tension between DODAB concentrations of 50 and 100 $\mu mol\,L^{-1}$ can be attributed to the formation of surfactant–polymer aggregates with greater surface activities than those of pure DODAB. The main interaction between DODAB and XAN is electrostatically driven: $DODA^+$ molecules bind to negative sites on XAN molecules in an ion-exchange process. However, this is not the only interaction possible; the alkyl tails of the surfactant can also bind to the polymer backbone through hydrophobic interactions, just as with GMC.

The binding of DODAB onto the negatively charged sites of XAN is an endothermic process driven by the entropy gain resulting from the release of condensed counterions. When condensed on XAN, counterions lose their translational entropy; this entropy is returned when DODAB is added and an ion-exchange occurs between the counterions and the $DODA^+$ molecules. This entropy gain is the essential driving force that causes the binding to proceed.

The XAN charge density also plays a major role in the DODAB–XAN interaction. According to Naves and Petri, raising charge density of anionic carboxymethyl cellulose increased the entropic gain in the interaction with cationic surfactant CTAB, due to counter-ions release (Naves & Petri, 2005).

As surfactants bind to the negative sites, the Coulombic repulsion between XAN molecules is reduced and due to barrier repulsion potential reduction, the tendency for them to flocculate/precipitate augments, as was observed macroscopically.

The interfacial tension increment observed between DODAB concentrations of 100 and 1250 $\mu mol\,L^{-1}$ may be due to the precipitation of surfactant–polymer aggregates, which creates hydrophobic domains in the bulk. It could also be due to desorption of surfactant monomers from the interface as they leave to bind to these clusters. A similar effect was observed by Viseu, Velázquez, Campos, García-Mateos, and Costa (2000) for cationic surfactants mixtures. The surface tension increase above the CAC was attributed to surfactant migration from the interface to the bulk. This interpretation was later supported by phase-contrast microscopy. In addition to the desorption of monomers from the interface, Manoli and Avranas (2013) demonstrated that surfactant–polymer clusters formed in the bulk between the CAC and the CVC hinder the adsorption of surfactant at the interface.

As more DODAB is added, XAN molecules lack the space to accommodate them; free surfactant molecules remain in the mixture and migrate to the drop interface, abruptly reducing the interfacial tension to its minimum at the critical vesicle concentration (CVC). Because of the higher CVC in XAN compared with the CVC of pure surfactant in ultrapure water, the XAN mixture reaches a plateau at a lower interfacial tension.

This result can be attributed to the ammonium head groups and the reduction of the Coulombic repulsion at the interface, mediated by Br^- ions, which occurs once fewer counterions are necessary to stabilize the surfactant–polymer clusters than to stabilize the pure surfactant vesicles. According to Jiang et al. (2013), this reduction can be attributed to the surfactant–polymer aggregates, which facilitate the adsorption of new surfactant molecules between the already adsorbed ones, thus increasing the number of surface-active species.

Above the CVC, the further addition of surfactant results in the formation of pure surfactant vesicles; the repulsion of the positive charges of the vesicles resuspend the surfactant–polymer aggregates.

At 1000 $\mu mol\,L^{-1}$ of DODAB in XAN there is a rise in the zeta potential of the aggregates (Fig. 1b), showing that the negative sites on the polymer are occupied by $DODA^+$. The initial interactions of DODAB and XAN can only reduce the negative charge at the occupied carboxyl sites. When the negative charges on the polymer are neutralized, the surfactant molecules then bind to the polymer backbone with hydrophobic interactions between the backbone and their alkyl tails; these interactions leave their ammonium head groups exposed and provide the aggregates with a positive charge.

Zeta potential analysis is a common method to determine the stability of colloidal systems. Usually, when the absolute zeta potential value is between −30 and +30 mV, particles tend to flocculate/precipitate (Li et al., 2011), as observed in the mixture of DODAB in XAN where precipitation occurred at values between −40 and -30 mV. The precipitation in this range can be understood because the charge measured is related only to the suspended, partially unbound XAN–DODAB molecules; the zeta potential analysis was measured with only the supernatant, and the aggregates were not considered.

Below the CVC, there are still XAN carboxyl sites unbound to $DODA^+$ molecules, which results in a superficial negative charge at 1000 $\mu mol\,L^{-1}$. Above the CVC, the system charge becomes positive and is approximately 30 mV, indicating the formation of free DODAB vesicles that stabilizes the system and explains the resuspension of the precipitated aggregates.

An enlargement in the diameter of DODAB aggregates with the addition of surfactant up to the CVC is also observed (Fig. 1c). Only the supernatant was analyzed, and the aggregates appeared to form clusters larger than 2000 nm. These clusters show a high level of light scattering and result in the high turbidity shown in Fig. 3. Above the CVC, it was only possible to determine the size of pure surfactant vesicles because of the system's high turbidity, as shown in Fig. 3, in comparison with the turbidity of the other systems.

At the CVC, the vesicle formation and adsorption thermodynamics of DODAB in XAN were similar to the thermodynamics of DODAB in ultrapure water (Table 2), which supports the idea that

all XAN molecules were saturated and that the polymer was no longer affecting the system. For this reason, the thermodynamic parameters of DODAB in XAN at the CVC did not receive much attention.

4.4. Comparison of the interactions of GMC and XAN with DODAB

Fig. 1b shows that in ultrapure water 100 μmol L^{-1} of DODAB is enough to form positively charged nanoparticles compared with 1000 μmoL L^{-1} of DODAB in a GMC solution and 10,000 μmol L^{-1} of DODAB in a XAN solution. This increase in the required DODAB concentration results from DODAB binding to the polymer molecules and providing them with its positive charge.

This analysis shows that surfactant molecules interact first with polymers and then with other surfactant molecules. Free surfactant vesicles are only formed above the CVC. If pure surfactant vesicles were formed below the CVC, there would be a bimodal zeta potential distribution with one highly positive peak related to the DODAB vesicles and another peak close to the polymers' own zeta potential.

The increasing diameter of the DODAB–XAN aggregates with the addition of surfactant molecules, as shown with DLS (Fig. 1c), shows the different interactions between the cationic surfactants and nonionic or anionic polymers. As DODAB and GMC interact hydrophobically, the surfactant's positive charges face outward, and the aggregates repel each other. The enlargement in aggregate diameter occurs only until free vesicles are formed, at which point the aggregates shrink from the Coulombic repulsions.

In the DODAB–XAN system with ion-exchange interactions, the alkyl tails face outward, which favors the formation of large clusters that can be suspended, floating or precipitated.

It is thermodynamically favorable for surfactant molecules to be at the interface rather than in the bulk. Approximately 80% of the surface has to be covered to initiate the self-aggregation of the surfactant into vesicles (Mukherjee, Moulik, & Rakshit, 2013). A more negative standard free energy of adsorption (ΔG^0_{ads}) relative to the standard free energy of vesicle formation (ΔG^0_{ves}) for DODAB (Table 2) shows that adsorption is more spontaneous than vesicle formation. Because in the GMC medium CAC and CVC were indistinguishable, the ΔG^0_{ves} corresponds to the sum of both aggregation and free vesicle formation. When compared to XAN, the sum of DODAB's ΔG^0_{ves} at the CAC and CVC, it is clear that the formation of vesicle and aggregation in XAN solution was more spontaneous.

However, in the solution of XAN, the adsorption was more pronounced at the CAC than in all of the other cases. According to Babak, Vikhoreva, and Lukina (1997), the increase of the free adsorption energy of the surfactant on binding to XAN could be explained with three main factors:

Neutralization of the electric charge on the head of DODAB by the oppositely charged functional groups of the XAN polymer, which reduces the repulsive electrostatic force to nearly zero, favoring the adsorption of DODAB to the interface and the formation of the adsorption layer;

Deeper immersion of the alkyl chains of the bound surfactant molecules into the nonpolar phase (air) owing to the electrical charge neutralization;

Adsorption of the hydrophobic fragments of the pyranose cycles of XAN at the air-water interface, which could not occur before the polymer bonded with DODAB molecules because of the high solubility of the XAN polymer.

The Γ_{max} measures the changes in the air/solution interface caused by surfactant adsorption. It depends on the adsorbed structure and its orientation at the interface. A lower Γ_{max} for DODAB-XAN at the CAC indicates that surfactant molecules were interacting with XAN molecules as described above. The a_{min} expanded in the presence of GMC and XAN at the CAC.

These results can be attributed to the compactness of the interfacial monolayer at the air/solution interface in the presence of GMC and XAN, which results from the finite presence of the solubilized DODAB–polysaccharide complex at the interfacial monolayer, as described by Chakraborty, Chakraborty, Moulik, and Ghosh (2009).

However, at the CVC of DODAB in XAN, both Γ_{max} and a_{min} were slightly lower than they were in ultrapure water, indicating that DODAB–XAN aggregates stabilized the adsorbed monomers at the interface and allowed more surfactant molecules to be adsorbed, forming a more compact monolayer, as described by Jiang et al. (2013).

Even though the enthalpy raises, aggregate formation is favorable, as shown by the negative ΔG^0_{ves}. This is because aggregate formation also increases the entropy of the whole system at 25 °C (Matulis, Rouzina, & Bloomfield, 2000; Wang & Tam, 2002; Wang, Tam, Jenkins, & Tan, 2003).

5. Conclusion

DODAB forms larger aggregates with XAN which interact with each other forming large micrometric clusters causing high turbidity and that precipitate when the zeta potential of the system becomes inferior to 30 mV. These precipitates can be resuspended with further addition of surfactant molecules, which associate in LUV's that stabilize the system by cationic Coulumbic repulsion. In GMC media the DODAB–polymer aggregates are smaller and uniform, with no precipitation and no observed turbidity even in high surfactant concentrations. Less DODAB is required to reach the minimal interfacial tension plateau in GMC than in XAN, however the plateau reached in XAN has a much lower interfacial tension. Both systems have their applicability, each of them with its benefits. The choice to use electrostatic or hydrophobic based surfactant–polymer interaction has to be thought of the system that is being built and its function.

Acknowledgments

We acknowledge the Brazilian funding agencies Conselho Nacional de Pesquisa (CNPq, no. 477275/2012-5), Fundação Araucária (FA no. 23643), Rede Nanobiotec (CAPES, Project 34). R.A.F, M.R.S and R.P. are research members of CNPq, G.A.T.K is a beneficiary of a scholarship from CAPES (REUNI). We are grateful to Dr. Tania Mari Belle Bresolin (UNIVALI) for the zeta potential analysis and Denise F.S. Petri (USP) for the scientific discussions.

Appendix A. Supplementary data

Supplementary data associated with this article can be found, in the online version, at http://dx.doi.org/10.1016/j.carbpol.2014.08.111.

References

Babak, V. G., Vikhoreva, G. A., & Lukina, I. G. (1997). Interaction between carboxymethylchitin and tetradecyltrimethylammonium bromide: Phase separation, surface tension and stability of microscopic foam films and foams. *Colloids and Surfaces A: Physicochemical and Engineering Aspects*, *128*, 75–89.

Bain, C. D., Claesson, P. M., Langevin, D., Meszaros, R., Nylander, T., Stubenrauch, C., et al. (2010). Complexes of surfactants with oppositely charged polymers at surfaces and in bulk. *Advances in Colloid and Interface Science*, *155*, 32–49.

Berg, J. C. (2010). *An introduction to interfaces and colloids the bridge to nanoscience*. Singapore: World Scientific.

Brito, R. O., & Marques, E. F. (2005). Neat DODAB vesicles: Effect of sonication time on the phase transition thermodynamic parameters and its relation with incomplete chain freezing. *Chemistry and Physics of Lipids*, *137*, 18–28.

Chakraborty, T., Chakraborty, I., & Ghosh, S. (2006). Sodium carboxymethylcellulose–CTAB interaction: A detailed thermodynamic study of polymer–surfactant interaction with opposite charges. *Langmuir*, 9905–9913.

Chakraborty, T., Chakraborty, I., Moulik, S. P., & Ghosh, S. (2009). Physicochemical and conformational studies on BSA–surfactant interaction in aqueous medium. *Langmuir*, *25*, 3062–3074.

Dakia, P. A., Blecker, C., Robert, C., Wathelet, B., & Paquot, M. B. D. A. (2008). Composition and physicochemical properties of locust bean gum extracted from whole seeds by acid or water dehulling pre-treatment. *Food Hydrocolloids*, *22*, 807–818.

Dal-Bó, A. G., Laus, R., Felippe, A. C., Zanette, D., & Minatti, E. (2011). Association of anionic surfactant mixed micelles with hydrophobically modified ethyl (hydroxyethyl) cellulose. *Colloids and Surfaces A: Physicochemical and Engineering Aspects*, *380*, 100–106.

Dea, I. C. M., & Morrison, A. (1975). Chemistry and interactions of seed galactomannans. *Advances in Carbohydrate Chemistry and Biochemistry*, *32*, 241–312.

Feitosa, E., Adati, R. D., Hansson, P., & Malmsten, M. (2012). Thermal and structural behavior of dioctadecyldimethylammonium bromide dispersions studied by differential scanning calorimetry and X-ray scattering. *Plos One*, 1–9.

Feitosa, E., Barreleiro, P., & Olofsson, G. (2000). Phase transitions in dioctadecyldimethylammonium bromide and chloride vesicles prepared by different methods. *Chemistry and Physics of Lipids*, *105*, 201–213.

Feitosa, E., Jansson, J., & Lindman, B. (2006). The effect of chain length on the melting temperature and size of dialkyldimethylammonium bromide vesicles. *Chemistry and Physics of Lipids*, *142*, 128–132.

Gulrez, S. K. H., Al-Assaf, S., Fang, Y., Phillips, G. O., & Gunning, A. P. B. D. A. (2012). Revisiting the conformation of xanthan and the effect of industrially relevant treatments. *Carbohydrate Polymers*, *90*, 1235–1243.

Jansson, P. E., Kennark, L., & Lindberg, B. (1975). Structure of the extracellular polysaccharide from *Xanthomonas campestris*. *Carbohydrate Research*, *45*, 275–282.

Jiang, R., Wang, Y., Yang, Y., & Lin, C. (2013). Equilibrium and dynamic surface tension of carboxymethylchitosan and alkyl trimethylammonium bromide mixtures. *Journal of Dispersion Science and Technology*, *34*, 22–31.

Li, F., Luan, Y., Liu, X., Xu, G., Li, X., Li, X., et al. (2011). Investigation on the aggregation behaviors of DDAB/NaDEHP catanionic vesicles in the absence and presence of a negatively charged polyelectrolyte. *Physical Chemistry Chemical Physics*, *13*, 5897–5905.

Manoli, S., & Avranas, A. (2013). Aqueous solutions of the double chain cationic surfactants didodecyldimethylammonium bromide and ditetradecyldimethylammonium bromide with Pluronic F68: Dynamic surface tension measurements. *Colloids and Surfaces A: Physicochemical and Engineering Aspects*, *436*, 1060–1068.

Manousakis, M., & Avranas, A. (2013). Dynamic surface tension studies of mixtures of hydroxypropylmethylcellulose with the double chain cationic surfactants didodecyldimethylammonium bromide and ditetradecyldimethylammonium bromide. *Journal of Colloid and Interface Science*, *402*, 237–245.

Matulis, D., Rouzina, L., & Bloomfield, V. A. (2000). Thermodynamics of DNA binding and condensation: Isothermal titration calorimetry and electrostatic mechanism. *Journal of Molecular Biology*, *296*, 1053.

Mukherjee, I., Moulik, S. P., & Rakshit, A. K. (2013). Tensiometric determination of Gibbs surface excess and micelle point: A critical revisit. *Journal of Colloid and Interface Science*, *394*, 329–336.

Naves, A. F., & Petri, D. F. S. (2005). The effect of molecular weight and degree of substitution on the interactions between carboxymethyl cellulose and cetyltrimethylammonium bromide. *Colloids and Surfaces A: Physicochemical and Engineering Aspects*, *254*, 207–214.

Rosen, M. J., & Aronson, S. (1981). Standard free energies of adsorption of surfactants at the aquous solution/air interface from surface tension data in the vicinity of the critical micelle concentration. *Colloids and Surfaces*, *3*, 201–203.

Viseu, M. I., Velázquez, M. M., Campos, C. S., García-Mateos, I., & Costa, S. M. B. (2000). Structural transitions in a bicationic amphiphile system studied by light-scattering, conductivity, and surface tension measurements. *Langmuir*, *16*, 4882–4889.

Wang, C., & Tam, K. C. (2002). New insights on the interaction mechanism within oppositely charged polymer/surfactant systems. *Langmuir*, *18*, 6484.

Wang, C., Tam, K. C., Jenkins, R. D., & Tan, C. B. (2003). Interactions between methacrylic acid/ethyl acrylate copolymers and dodecyltrimethylammonium bromide. *Journal of Physical Chemistry B*, *107*, 4667–4675.

Wu, F. G., Yu, Z. W., & Ji, G. (2011). Formation and transformation of the subgel phase in dioctadecyldimethylammonium bromide aqueous dispersions. *Langmuir*, *27*, 2349–2356.